ing of hydrogen lines in plasma," National Research Lab Rept 5455 (March 1962)

[4] Unsöld, A , ' Continuous spectrum of high-pressure Hg lamp and similar gas discharges," Ann Physik **33**, 607–616 (1938)

[5] Biberman, L M and Norman, G E , "On the calculation of photoionization absorption," Opt i Spektroskopiy **8**, 433 (1960); also Opt Spectr (USSR) (English Transl) **8**, 230 (1960)

[6] Fay, J A and Kemp, N H , "Theory of stagnation point heat transfer in a partially ionized diatomic gas," Avco-Everett Res Lab Res Rept 144 (April 1963)

A Flow-Separation Spike for Hypersonic Control of a Hemisphere-Cylinder

WILLIAM E THURMAN*
Aerospace Research Laboratories, Wright Patterson Air Force Base, Ohio

Nomenclature

L/D = lift/drag
Re = Reynolds number based on the body diameter and the free stream conditions ahead of the body
s/d = longitudinal arc length measured from the centerline of the body/the diameter of the body
β = reattachment angle measured from the longitudinal centerline of the body, deg
θ = spike deflection angle measured from the centerline of the body, deg
ϕ = angle of each longitudinal ray measured from the direction of the spike deflection clockwise from the front, deg

Introduction

THERE has been considerable interest in the study of hypersonic flows in which a separated region is induced ahead of the body by a flow-separation spike Bogdonoff and Vas[3] were among the first investigators to determine that the spike reduces the form drag and, if the flow remains laminar, lowers the over-all heat transfer to the forebody These results suggest that the spike may have flight applications

The present study investigates the possibilities of using a deflected flow-separation spike to control a body at hypersonic speeds It is a preliminary investigation in that one body shape is tested at only one Mach number and Reynolds number The study determines the lift and drag coefficients that result from the changing spike deflections These coefficients were obtained by integrations of the surface pressures

Experimental Facilities and Model

The experimental investigation was concluded in the Aerospace Research Laboratories' 3-in hypersonic wind tunnel A conical, nominal Mach 12 nozzle that had a Mach number gradient of 0 42/in along the centerline of the open-jet test section was used for the study

The stainless-steel model is schematically shown in Fig 1 It consisted of a right circular-cylindrical afterbody $\frac{1}{2}$ in in diameter, with a hemispherical nose A flow-separation spike, $\frac{1}{16}$ in in diameter, with a spike length to body diameter ratio of 4, extended ahead of the nose of the body This spike length was determined by the authors of Ref 3 to be the optimum spike length for decreasing both the form drag and the over-all heat transfer to the model The model was

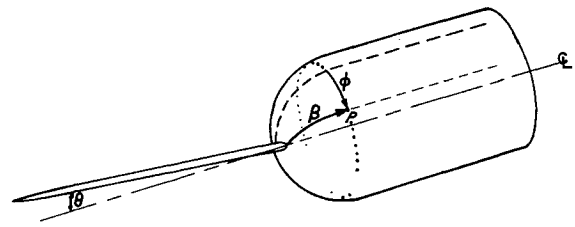

Fig 1 The test model showing angular measurements

equipped with 10 pressure orifices located at various spiral positions about its surface

A double-pass Schlieren system and glow discharge flow-visualization techniques were used for visual studies of the flow field

Test Program

In these studies the centerline of the model was aligned with the centerline of the wind tunnel Only the spike was deflected through an angle that was measured from the centerline of the model The test program was designed to measure in detail the pressure distribution over the model which resulted from the spike deflection Accurate measurement of this pressure distribution required a large number of pressure readings on the body surface, but the maximum number of orifices that could be placed in the model was limited to 10 Therefore, the model was designed with fixed deflection spikes that could be rotated through 360° about the longitudinal axis of the model The model was fixed and the spike rotated

Pressures were recorded as the spike was rotated through 360° in increments of 20° This afforded 180 pressure readings to use for the pressure integration Pressure distributions were measured with 0 spike deflection and with spike-deflection angles measured from the centerline of the model of 47° 5′, 2° 30′, 4° 58′, and 7° 15′

The Reynolds number of the test remained constant at 28,700/in [2] A test Mach number of 11 76 was used with stagnation conditions of 400 psia and 1300°F Although these stagnation conditions might result in air condensation in the test section, a report by Daum[5] indicated that liquefaction did not occur

The longitudinal Mach number gradient along the tunnel centerline was not considered important to the results of this study since 8 of the 10 pressure orifices were within 0 25 in of the spike base Therefore, a Mach number of 11 76 was used for this study This Mach number corresponded to the location of the spike base The choice of a constant Mach number for data reduction did not introduce appreciable errors in the computations of the force coefficients

Pressure Measurements

Examples of some of the curves of pressure distribution that were measured in these tests are given in Fig 2 which shows the curves of the pressure distribution for each spike-deflection angle along the longitudinal ray opposite to the direction of the spike deflection Also plotted in this figure is the pressure distribution along a longitudinal ray for the straight spike and the modified Newtonian pressure distribution over the hemispherical nose of the body

The shape of the pressure distribution curve for the straight spike is similar to the curve shapes obtained by the authors of Ref 3 at Mach 14 in helium The individual pressure values measured along the model during the present tests are higher than the pressures measured by Bogdonoff and Vas, but these sets of data cannot be accurately compared because the tests were made in a different testing medium and at a different Reynolds number

The pressure distribution curves that were obtained by Crawford[4] are similar to the straight spike pressure distribution curves that were measured in these tests A comparison

Received October 2, 1963

* Captain, U S Air Force, and Research Aerospace Engineer, Hypersonic Research Laboratory

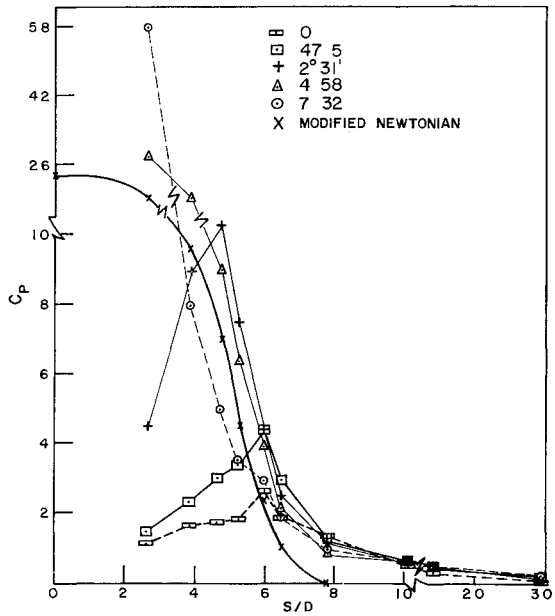

Fig 2 Pressure distributions along the longitudinal ray opposite to the spike deflection for the various spike deflections

of individual pressure values cannot be made since they were taken at a different Reynolds number and Mach number Crawford's report shows that these pressures are a strong function of the Reynolds number

The curves on Fig 2 of the pressure distribution for the deflected spike have the same shape as the pressure distribution curves for the straight spike However, the individual values of pressure on the hemispherical nose of the body are much higher The peak pressure for each curve occurs near the position of reattachment Therefore, an indication of the change of the reattachment position along the 180° longitudinal ray with increased spike deflection can be seen by observing the change in the position of peak pressure The reattachment position on this longitudinal ray moves, as should be expected, toward the spike base as the spike is deflected through higher angles of attack

The pressures downstream of reattachment are higher than the corresponding pressures given by the modified Newtonian theory This can be seen for one longitudinal ray in Fig 2 The highest pressure that was measured for any spike deflection increased with increased spike-deflection angles until, at the largest spike deflections, the pressures at reattachment were about three times the normal shock recovery pressure

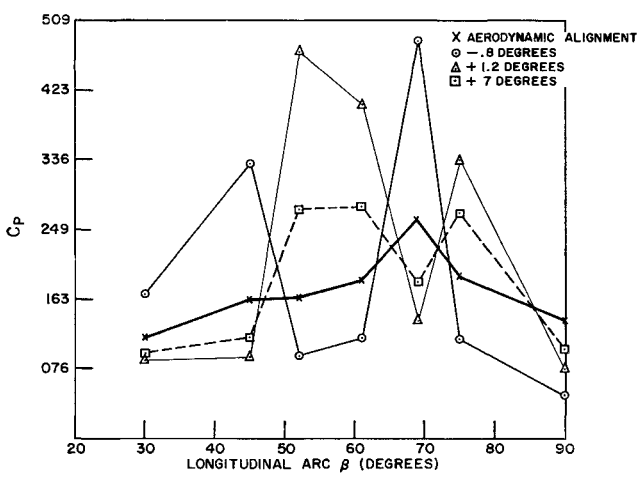

Fig 3 Pressure distribution change with misalignment for a straight spiked model

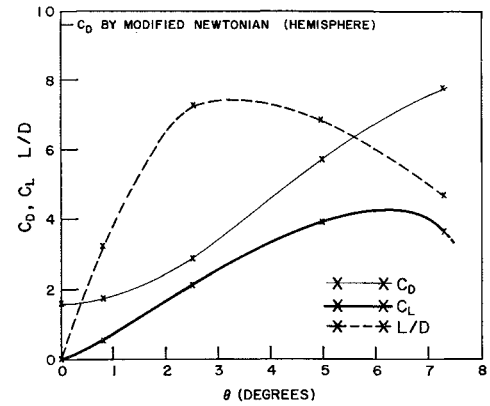

Fig 4 Lift, drag, and L/D vs spike-deflection angle

These higher pressures resulted from the recompression through the oblique shock waves caused by the flow disturbance of the spike and the model

The afterbody pressures, as can be seen in Fig 2, are relatively unaffected by the changing spike deflections

The reattachment position on the model equipped with a straight spike was determined through pressure distribution and Schlieren photography to be near 69° This reattachment position corresponded quite closely to the reattachment position of about 75° that was found by both Bogdonoff and Crawford

It became apparent in the course of this study (see Fig 3) that the measured pressures are very sensitive to model alignment in the tunnel For the straight spike, the peak pressure was changed by 50%/deg of misalignment This occurred because the small change in the body position in the tunnel caused the reattachment to shift so that the orifice no longer measured the reattachment pressure A note has been submitted by Album[1] in which he discusses the alignment problem and shows the sensitivity of the pressure readings with alignment

The shape of the pressure curves found in Ref 6 are similar to the pressure curves obtained in this study when the model was misaligned This suggests that Stalder's and Nielsen's models might have been misaligned and emphasizes the importance of correct alignment when spiked body-pressure surveys are being taken

Pressure Integration

The coefficients of lift and drag were obtained by an integration of the pressure distribution over the model surface The pressures in the vicinity of the spike base were assumed to be the separated region pressure This assumption affected the values of the force coefficients by less than 7% Base pressures were not considered in the computations The force coefficients are plotted in Fig 4

The drag coefficient was reduced to 16% of the modified Newtonian pressure drag coefficient of a hemisphere by the addition of a straight spike This value of drag is 34% higher than the corresponding drag of Ref 3 and 27% higher than the corresponding drag of Ref 4 As the spike was deflected from the centerline, the value of the drag coefficient increased rapidly At 7½° of spike deflection, the largest deflection investigated, the pressure drag was about 81% of the modified Newtonian pressure drag for a hemisphere-cylinder without a spike

The deflected spike produced a lift coefficient that attained a maximum value near 6° of spike deflection It is important to note that the lift coefficient is of the same order of magnitude as the drag coefficient throughout the range of spike deflections that were tested

The curve of lift vs drag is also plotted in Fig 4 The maximum L/D occurs at about 3 3° of spike deflection and then decreases for larger spike deflections

The values of the lift and drag coefficients that are plotted in Fig 4 do not include the contribution of the spike itself The lift that could be obtained from the deflected spike alone was computed theoretically using Newtonian theory for the part of the spike forward of the separation point for all spike deflections The lift coefficient was found to be less than 4% of the lift coefficient which resulted from the changing pressure distribution over the body Since this value was small, it was neglected in this study

Conclusions

These tests were conducted at one Mach number and one Reynolds' number, and the problems of a high enthalpy Mach 12 flow have not been considered Subject to these restrictions, one may conclude the following: 1) the flow-separation spike can, when deflected, cause forces in the direction of the spike deflection of the same order of magnitude as the drag; 2) the maximum L/D and the maximum lift that result from the deflected spike occur at small angles of spike deflection barring any unexpected effects at large spike-deflection angles; and 3) accurate pressure distributions on the surface of the model can only be obtained if the model is aerodynamically aligned in the tunnel since small amounts of misalignment can greatly alter the measured pressure distribution

References

[1] Album, H H , "Flow and inclination measurements in hypersonic tunnels," submitted for publication in AIAA J

[2] Ames Research Staff, "Equations, tables, and charts for compressible flow," NACA Rept 1135 (1953)

[3] Bogdonoff, S M and Vas, I E , "Preliminary investigations of spiked bodies at hypersonic speeds," Wright Air Dev Center TN 58-7 (AD 142 280) (March 1958)

[4] Crawford, D H , "Investigations of the flow over a spiked-nose hemisphere-cylinder at a Mach number of 6 8," NASA TN D-118 (December 1959)

[5] Daum, F L , "Air condensation in a hypersonic wind tunnel," AIAA J 1, 1043–1046 (1963)

[6] Stalder, J R and Nielsen, H V , "Heat transfer from a hemisphere cylinder equipped with flow-separation spikes," NACA TN 3287 (September 1954)

Boundary of Underexpanded Axisymmetric Jets Issuing into Still Air

A F CHARWAT*
University of California, Los Angeles, Calif

THE boundaries of an underexpanded axisymmetric jet issuing supersonically into still air can be calculated by the method of characteristics,[1] but since that is a lengthy procedure, empirical formulas[2] and approximate analytical models have been sought In particular, Adamson and Nicholls[3] and also Love[4] calculated the shape of the free jet in the initial region by requiring that the external streamtube undergo sufficient compressive turning to cancel the local pressure gradient due to area expansion They estimated this gradient from the rate of increase of the local radius of the jet, implying that the flow throughout the jet core is quasi-one-dimensional

A more satisfactory and apparently more accurate model explores fully the fact that the flow along the jet boundary is nearly isentropic, at least initially (turning-compression waves are weak) Under this assumption the jet-edge Mach number is determined entirely by the corner expansion to ambient pressure and remains constant along the jet boundary, together with the associated isentropic flow functions such as the stagnation pressure P_t and the local sonic throat area A^*

Following a procedure similar to that of Ref 3, the condition that the static pressure on the free jet boundary be constant is written as

$$d\left(\frac{P}{P_t}\right) = \frac{\partial(P/P_t)}{\partial(A/A^*)}\frac{dA}{A^*} + \frac{\partial(P/P_t)}{\partial\theta}d\theta \tag{1}$$

$$\frac{dA}{A^*} = 2\left(\frac{A_j}{A^*}\right)\left(\frac{r}{r_j}\right)d\left(\frac{r}{r_j}\right) \tag{2}$$

$$\frac{\partial(P/P_t)}{\partial\theta} = \frac{\gamma_j M^2(P/P_t)}{(M^2-1)^{1/2}} \tag{3}$$

Define a function ψ which according to the present model is a constant along the jet boundary (in contrast with the model of Ref 3):

$$\psi = \frac{\partial \ln(P/P_t)}{\partial(A/A^*)}\frac{A_j}{A^*}\frac{(M^2-1)^{1/2}}{\gamma_j M^2}$$

It can be expressed as follows, using isentropic flow relations,

$$\psi = \frac{2}{\gamma_j+1}\frac{(M^2-1)^{1/2}}{M^2(A/A^*)_M}\left(\frac{A}{A^*}\right)_{M_j} \tag{4}$$

In the forementioned, the area ratios $(A/A^*)_M$ could be written out in terms of Mach number (which is indicated by the subscript) or in terms of the pressure ratios, but they are more conveniently evaluated by the use of compressible flow tables

After integration, Eqs (1–4) yield the following relation:

$$\theta - \theta_0 = \psi[1 - (r/r_j)^2] \tag{5}$$

θ_0 is the initial expansion angle at the edge of the nozzle, which is known in terms of the Prandtl-Meyer function and the nozzle divergence half-angle at the exit:

$$\theta_0 = \nu_M - \nu_{Mj} + \theta_j \tag{6}$$

From Eq 5, the shape of the jet boundary in proper generalized coordinates is

$$X = \int_{1/\rho_0}^{R} \cot g[\phi(1-R^2)]dR \tag{7}$$

where

$$X = x/r_j\rho_a \qquad R = r/r_j\rho_a \tag{8}$$

with the following two scale-parameters:

$$\rho_a = r_a/r_j = [1 + (\theta_0/\psi)]^{1/2} \tag{9}$$

$$\phi = \psi\rho_a^2 = (\psi + \theta_0) \tag{10}$$

Equation (7) is easily integrated numerically Figure 1 shows several of the generalized jet boundaries with ϕ as a parameter (see also Fig 3) The second parameter ρ_a enters through the definition of the real origin of the free jet (edge of nozzle) X_0, relative to the virtual origin $X = 0$, where

$$X_0 = [X \text{ at } R = 1/\rho_a] = \int_0^{1/\rho a} \cot g[\phi(1-R^2)]dR \tag{11}$$

The shape of the jet boundary is specified by the *two* generalized parameters ϕ and ρ_a, which contain the influence of the *four* physical parameters M_j, θ_j, (P/P_j), and γ_j

Figure 2 shows a comparison of the present analysis with a specific calculation by the method of characteristics[1] and the model of Adamson and Nicholls [3] The results are seen to be remarkably good

The scale factor ρ_a is, formally, the ratio of the asymptotic radius of the free jet boundary to the nozzle exit radius r_j

Received October 15, 1963

* Professor, Department of Engineering Member AIAA